



7th International Conference on Fatigue Design, Fatigue Design 2017, 29-30 November 2017,
Senlis, France

Fatigue crack growth in welds based on a V-notch model for the short crack propagation at the toe

Naman Recho^{1,2}, *Tom Lassen*³ and *Oyvind Ness Mikkelsen*³

¹ERMES, EPF – Ecole d'ingénieurs, 3 bis, rue Lakanal, 92330 Sceaux-France

²University Clermont Auvergne, Pascal Institute, CNRS, UMR 6602, PB 10448, 63000, Clermont-Fd, France

³University of Agder, Lilltunsvei 9 N-4879 Grimstad, Norway

Abstract

This work presents a new fatigue crack growth prediction model for non-load-carrying fillet welded steel joints. For this joint configuration the fatigue cracks will emanate from the weld toe region. Due to the presence of a V-notch in this region the crack initiation point becomes a point of singularity for the stress field. This may in many cases make it difficult to determine the Stress Intensity Factor Range (SIFR) for small cracks by conventional methods based on Linear Elastic Fracture Mechanics (LEFM). The present approach solves this problem by using the Energy Release Rate (ERR) to determine the SIFR in the small crack growth regime. The model is fitted to crack growth curves from tests with cruciform steel welded joint subjected to constant stress ranges in both axial and bending loading mode. The Paris crack propagation law is adopted and the calculation of SIFR for larger cracks outside the material volume influenced by the V-notch singularity is carried out by the conventional approach. The model gives results in agreement with experimental facts and has also the potential of being extended to variable amplitude loading. The model is also well suited for taking into account the crack initiation phase that is significant for high quality welded joints

© 2018 The Authors. Published by Elsevier Ltd.

Peer-review under responsibility of the scientific committee of the 7th International Conference on Fatigue Design.

Keywords: Fatigue, Fracture mechanics, Welded joints, Energy release rate, V-notch

I- Introduction and Development:

Modeling the evolution of the fatigue damage in welded steel joints is an important issue for the design of dynamically loaded structures. In fillet welded joints cracks often emanate from the weld toe and subsequently grow through the plate thickness. Common approaches to model the damage process are an application of rules based on S-N curves for life predictions and a fracture mechanic model to describe the associated crack growth in more detail. The latter approach has the disadvantage that the modeling of small crack growth in high quality welded joints often is outside the validity range of Linear Elastic Fracture Mechanics (LEFM) theory. The initial crack size is generally unknown. Furthermore, the necessary calculation of the Stress Intensity Factor Range (SIFR) at these small crack depths may be difficult. The limitations are due to the fact that the singular behavior at the point defined by the weld to transition to the plate surface has a great influence on the SIFR calculations. Also the theoretical significance of the SIFR is to be under question. In the present paper, we study the fatigue behavior of fillet welded joint in which the principal significant parameter to calculate the stress intensity factor is the weld toe angle.

In many standards, as the Eurocode 3, the approach to design fatigue life of the welded joints is based on hot spot stresses that takes into account the global stress concentration. But, many studies show that this approach is not precise and overestimates the fatigue life of the joint. The fatigue life of a cracked V-notch structure can be divided into three parts (Recho, 2010): the crack initiation part, the crack propagation part until the singularity of the V-notch has no influence on the crack growth and finally the crack propagation part with no V-notch influence.

On this background the present study proposes a new two-phase model for the fatigue damage evolution in fillet welded joints (Lassen, Recho 2009). The first phase models the two first parts described above. The micro crack behavior is based on the calculation of the Energy Release Rate in the V-notch region at the weld toe to obtain an equivalent SIFR (Cheng, Recho et al. 2011). This gives substantial different results compared to classical fracture mechanics.

When the material volume beneath weld toe that is influenced by the singular V-notch behavior is passed the present approach will give results very close to the classical fracture mechanics model. This constitutes the second phase of the damage process. Both phases are adopting the Paris exponential law for the crack growth rate. The empirical parameters are fitted to experimental fatigue tests of cruciform steel welded joints subjected to axial loading mode under constant amplitude loading. When the measured crack growth rate is plotted against the equivalent SIFR, two slopes appear on the curve. The first slope corresponds to the short crack growth regime in phase 1 whereas the second slope characterizes the stable crack propagation in phase 2.

The aim of this paper is twofold. The first one consists in how determining the variation of the Energy Release Rate (E.R.R.) at the V-notch constituted by the weld toe at which a short-crack tip is close to the weld toe. This will be a major parameter allowing determining an equivalent stress intensity factor which will be used in the crack propagation during the first phase. The second objective is to determine the characteristic crack depth at which no influence of the V-notch is considered. That will be done on the basis of experimental results of crack depth as function of the number of cycles. A change of crack growth rate is observed at low values of crack depth. In order to evaluate the influence of this approach on the fatigue life, two specimen configurations are considered:

1. A V-notch specimen submitted to bending fatigue loading (Figure 1) the so-called three points bending beam;
2. A cruciform welded joint submitted to axial and bending fatigue loading (Figure 2).

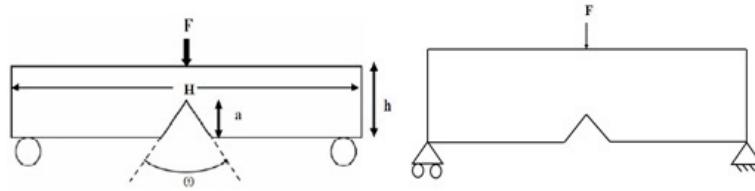


Figure 1 - Geometry specimen definition (left) and schematization of three point bending beam (right)

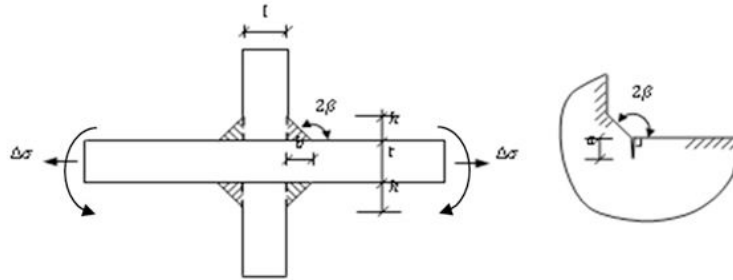


Figure 2 - Definition of specimen and toe geometry for a fillet welded joint

Moreover, it is necessary to find a numerical method to compute the Energy Release Rate (ERR) at the weld toe geometrical discontinuity modeling it like a V-notch angle in the continuum of the structure. Going from this computation, the fatigue life of the welded structure is determined by the use of a specific crack propagation law as described in the next section of this paper. A classical approach is considered in order to be compared with the present approach. It's based on the work given by Gurney (Gurney and Maddox 1973). In this classical approach, the initial depth is determined on the basis of experimental results given by Lassen (Lassen 1990) in order to obtain the same fatigue life duration. The present approach introduce the initial crack depth in a new calculation procedure (Cheng, Recho et al. 2011) allowing to determine the Energy Release Rate (G) for short crack emanating from V-notch. Finally, the results from the present approach are compared with results from the classical one. For the two approaches, the determination of the initial crack depth is associated to large uncertainties. Nevertheless, most of the fatigue life depends on this crack depth. Many investigations show that the influence of the initial crack depth on the fatigue life of the structure is important (Nykänen, Marquis et al. 2007, Goyal and Glinka 2013, Carpinteri and Paggi 2014). On the basis of 42 test specimens submitted to constant amplitude loading Lassen (1990) shows that the statistical initial crack distribution is dominated by small cracks with a mean value as small as 0.043 mm. This initial crack depth is determined by forcing the crack growth life to coincide with the S-N curve based life for a category 71 in the Eurocode. See **Table 1** below:

Table 1 – Crack growth model data for joints in air

Variable	Mean value	Standard deviation	Distribution type
a_0 [mm]	0.043	0.043	Exponential
M	3.0	fixed	-
LogC [MPa, m]	-11.24	0.11	Normal

In fact, approximately 30% of the fatigue life is spent before a crack depth of 0.1 mm is reached for a stress range of 150 MPa. Hence, the initiation phase plays an important role even at a high applied stress range.

II- Evaluation of the Stress Intensity Factor taking into account a V-notch tip

For a V-notched structure with an opening angle 2β and a polar coordinate (see Figure 3), the displacement and stress fields can be given by the following expressions (Seweryn,1998):

$$u_i(r, \theta) = \sum_{k=1}^N A_k(\theta) r^{\lambda_k + 1} \tilde{u}_{i,k}(\theta) \quad (i = r, \theta) \tag{1}$$

$$\sigma_{ij}(r, \theta) = \sum_{k=1}^N A_k(\theta) r^{\lambda_k} \tilde{\sigma}_{ij,k}(\theta) \quad (ij = rr, \theta\theta, r\theta) \tag{2}$$

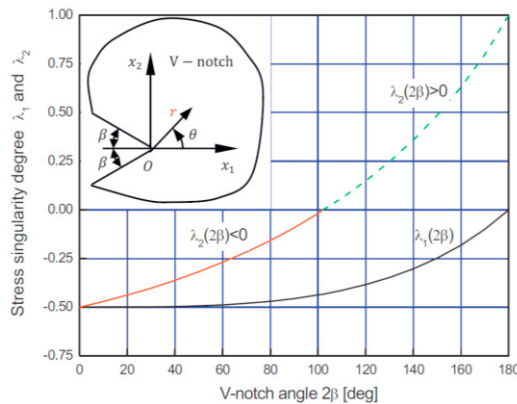


Figure 3 – First two singularity degrees of a V-notched structure

Where A_k are the amplitude coefficients, $\tilde{u}_{i,k}$ and $\tilde{\sigma}_{ijk}(\theta)$ angle functions and N the number of the truncated eigenvalues.

The first singularity degree has no significant difference until 2β is equal to 60° since it respects the singularity of the crack ($\lambda = -0.5$). That means the computation of K_I for a V-notched structure is the same than the cracked specimen. For opening angle higher than 80° , it can be noted the first singularity degree is greater than -0.5 and moves closer to zero (which corresponds to the case of a detail without any crack present). So the calculation of the SIF is affected by the effect of the V-notch especially by the opening angle and by the depth of the V-notch.

Numerical model

The two specimens simulated are shown in Figure 4 and Figure 5. The fatigue stress range $\Delta\sigma$ is 150 MPa, the specimen width is 40 mm and the specimen length is 200 mm. 2β and l represent respectively the opening angle and the depth of the V-notch. In Figure 5, the crack depth (a) corresponds to the sum of the initiated crack l_0 and the V-notch depth (l) of the Figure 4.

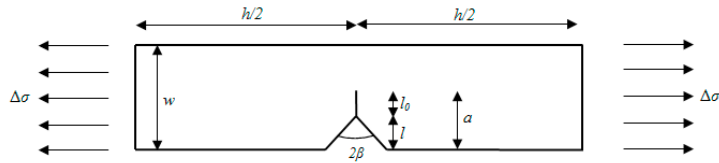


Figure 4 – Crack initiated from the notch tip in V-notched specimen

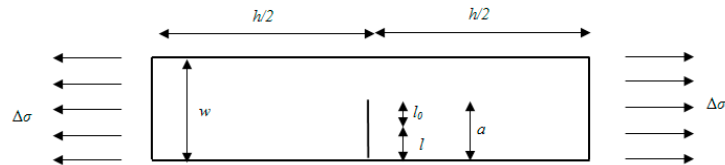
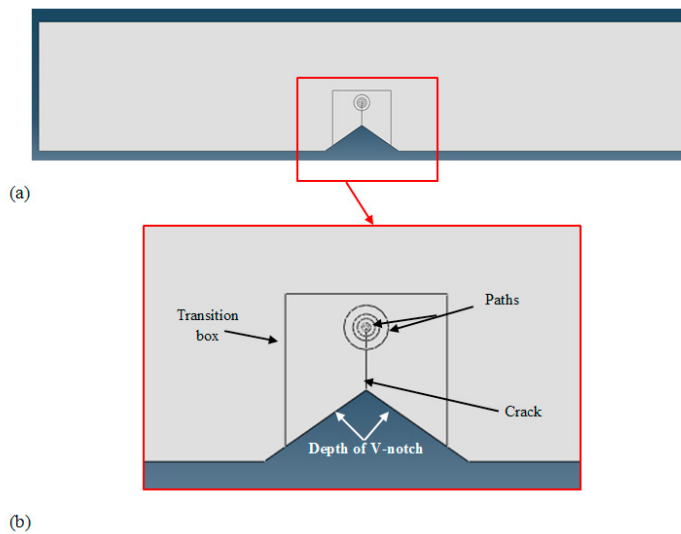
Figure 5 – Cracked specimen with $2\beta = 0^\circ$ 

Figure 6 – (a) V-notch structure (b) enlargement of the initiated crack from the notch tip in V-notch

Figure 6 shows the configuration of the “notch box” used in the numerical simulations of the specimen performed using the Abaqus software. Figure 6-b is an enlargement of the Figure 6-a showing the detail of the “notch box” which allows the mesh to be more regular. Moreover, 6 paths at the crack tip are used to verify the stability of the computation of the J integral given by Abaqus. In fact, it is demonstrated that the computation of the J integral provided by Abaqus is of good accuracy (Lebaillif 2006).

It's to be noted that the calculation of J values between 0.1 and 3mm crack depth are determined on the basis of the work done by (Cheng, Recho et al. 2011). In this work, a B.E.M. (Boundary Element Method) is developed. It allows, in elastic 2D plane strain state, to determine an equivalent Stress Intensity Factor for short cracks existing in the vicinity of the V-notch root. Also, for short crack depth close to the V-notch vicinity, the influence of V-notch is taking into account to determine the equivalent ΔK .

Numerical results

In this section, the study deals with the influence of two parameters concerning the V-notch: the opening angle and the depth of the V-notch. The stress intensity factor is calculated with the J integral as in the plane strain state:

$$K_I = \sqrt{\frac{JE}{(1-\nu^2)}} \quad (3)$$

Influence of the opening angle 2β of the V-notch

Figure 7 shows the SIF as function of different crack depths (0.1mm, 0.2mm and 0.5mm). For various opening angles, it can be stated that a large scatter exists when the crack depth is small. Consequently, a great change in fatigue life is expected.

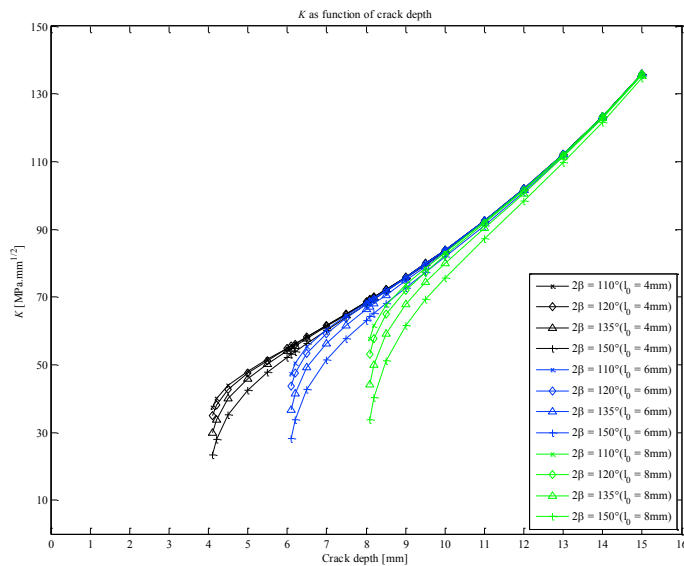


Figure 7 – SIF of cracks initiated at the V-notch tip with different crack depth l_0 varying between 4mm and 8mm

Moreover, larger is the initiated crack depth, larger is a scatter between SIF's values. For an unchanged notch depth, each plot tends to prove that there is a crack depth at which the V-notch has no more influence on the calculation of the SIF. It is called the characteristic crack depth a_c .

Influence of the depth l_0 of the V-notch

For an unchanged opening angle, Figure 8 presents SIF's values as function of the crack depth for different V-notch depth compared to the real crack configuration. The opening angles of the V-notch chosen are 110° , 120° , 135° and 150° because they represent the opening angle for the case of the cruciform welded joints (the weld toe angle studied in the paper is 45°).

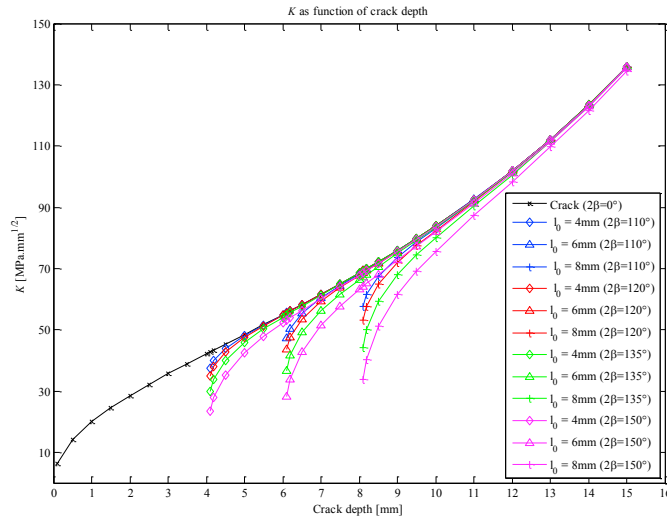


Figure 8 – SIF values of cracks initiated with opening angle varying between 110° and 150° compared with one equal to zero (the crack case)

The greater the opening angle of the V-notch and the greater the V-notch depth, the greater the SIF values decrease for small crack depth. Also, the greater the opening angle, the greater the difference between the cracked case and the V-notch case.. This shows the major influence of the V-notch parameters on the calculation of the SIF.

Characteristic crack depth

According to the previous sections, it is possible to determine a characteristic crack depth at which the influence of the V-notch vanishes. Figure 9 shows characteristic crack depths as function of the V-notch opening angle for different V-notch depths.

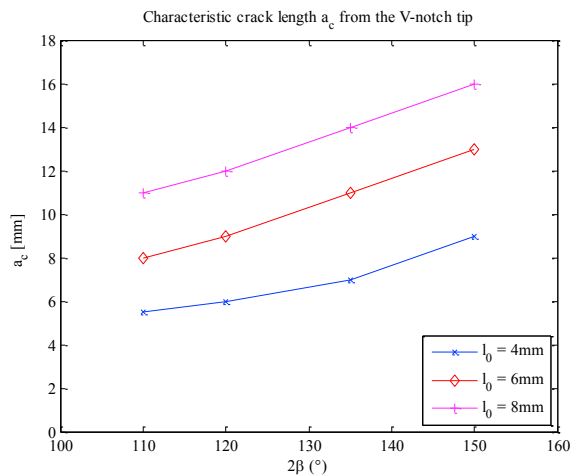


Figure 9 – Characteristic crack depth from the V-notch tip for different V-notch depth

III- Application to crack growth in cruciform welded joints

The present V-notch model is applied to pursue the experimental results obtained for cruciform welded joints of the type presented in Figure 2. As discussed the V-notch effect for this case is related to the local weld toe geometry parameters. The parameters in the model are chosen such that the calculated crack growth gives a good fit with the experimental curves.

Description of test specimens and test set-up

The tests are carried out with cruciform welded joints with dimensions as shown in **Figure 10**. The stresses are applied on the horizontal main plate transverse to the non-load-carrying fillet welds. The specimens were subjected to tensile loading mode.

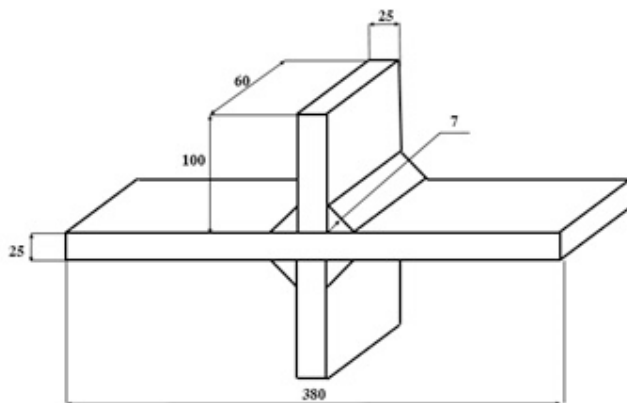


Figure 10 – Test specimen with dimension [mm]

The steel is a typical steel of off-shore North Sea platforms, a low carbon and accelerated cooling one. It has an elastic stress limit equal to 416MPa and a tensile strength of 501MPa (Lassen 1990). The measured mean fatigue life is quite close to category 71 in the Eurocode 9.

Four welding procedures are used:

- SAW (Submerged Arc Welding);
- FCAW (Flux-Cored Arc Welding);
- SMAW (Shielded Metal Arc Welding) 57 and 76.

The experimental results are particularly interesting because the early small crack growth that is subject to the present investigation was measured by high accuracy by an Alternating Current Potential Drop (ACPD) technique capable of revealing the formation of a crack with 0.1 mm depth. Test characteristics are given by:

- 42 specimens tested;
- Applied stress range of 150MPa;
- Effective stress ratio of 0.5;
- Frequency of applied stress 8Hz;
- Strain gauges located at distance 10mm from the weld toe;
- AC current 6kHz with associated monitoring system;
- Tests are done at normal laboratory conditions.

Experimental measured crack growth

In **Figure 11**, the crack depth as function of the number of applied cycles is plotted for each of the test specimens. Statistics concerning the crack depth and the number of cycles at failure are presented in **Table 2**. For the tensile loading mode it was an important observation that the mean time to reach a crack depth of $a=0.1$ mm was close to $1.45(10)^5$ cycles, i.e. 30% of the total fatigue life. This demonstrates that the initial crack depth is smaller than 0.1 mm and that early crack growth plays a significant role in the fatigue life. Further details are found in Lassen (1990). The accuracy of the depth measurements for early crack growth is shown in Figure 12. As can be seen there are reliable depth measurements down to 0.05 mm, but with some influence of noise from the very beginning. This is a typical trend for all specimens. After having passed 0.1 mm the signals become much more stable. Nevertheless, the measurements in figure 12 before a crack depth of 0.1 mm give a clear indication of the behavior of the crack at an early stage.

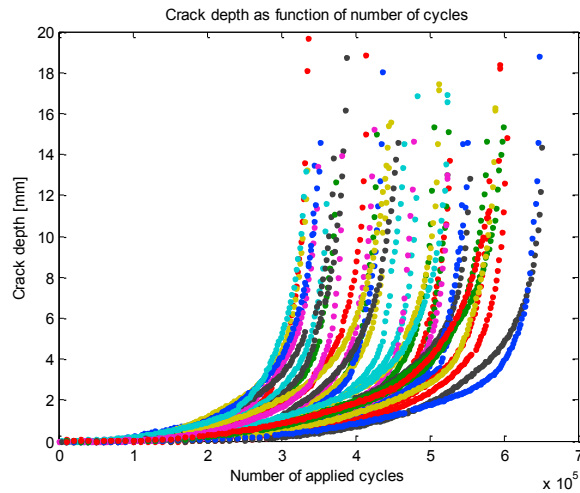


Figure 11– Crack depth as function of number of cycles – tensile loading test

Table 2 - Statistical analysis of experimental results at failure

Load	Statistics	Crack depth at failure [mm]	Number of cycles to failure
Tensile	Mean	15.16	$4.740 \cdot 10^5$
	Median	14.67	$4.717 \cdot 10^5$
	Std. deviation	2.00	$9.588 \cdot 10^4$

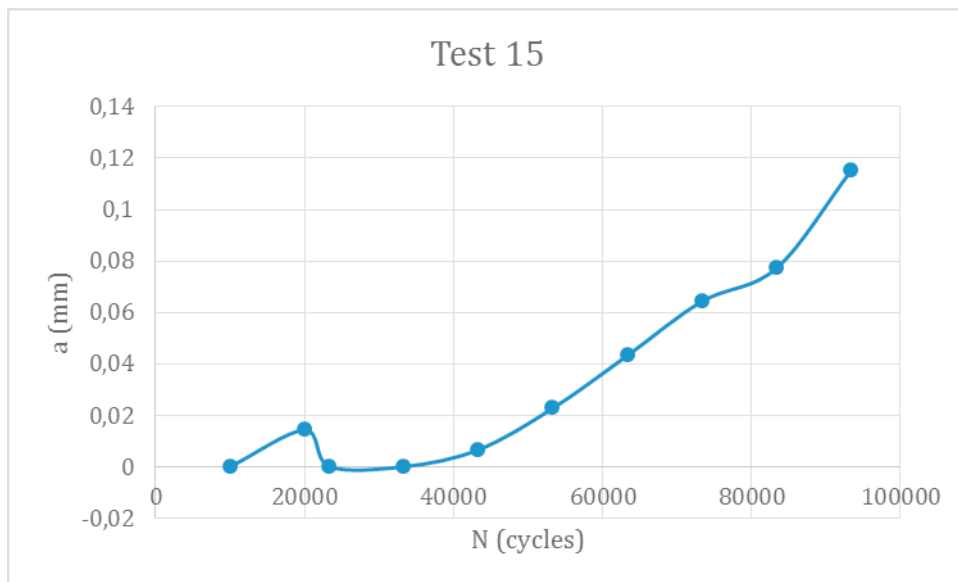


Figure 12-Measured early crack growth before reaching $a=0.12$ mm.

Modeling the measured crack growth by the present V-notch approach

Determining the geometry function and associated SIFR

In order to apply our approach, several crack depths are considered in order to compute the J-Integral (=ERR) and subsequently determine the SIF. The value which corresponds to the J-integral is the mean value between three contours at 1, 1.5 and 2.5mm from the crack tip. Within this zone, the J-integral value is almost stable.

Figure 13 shows the finite element mesh (half of the whole model) which is used. In fact, the symmetry condition along the y axis is considered. The model considers a plane strain state with an edge crack of depth a . Also, an equivalent K values has been deduced from the J-Integral. Values issued from our procedure are shown in Table 3 for tensile loading case. According to Figure 9, by extrapolation, one deduces that the characteristic crack depth is equal to 8mm.

It's to be noted that the calculation of J values between 0.1 and 3mm crack depth are determined by BIE (Boundary Integral Equations) analysis on the basis of the work done by (Cheng, Recho et al. 2011). In this work, the ratio between $\Delta K_v / \Delta K_c$ is giving following the **Figure-14**. ΔK_v is the variation of the SIF determined for a crack emanating from a V-notch, at 2β is equal to 135° and ΔK_c is the variation of the SIF determined for a crack where 2β is considered as equal to 110° (for this angle, no influence of weld toe is observed (for 2β see figure 2).

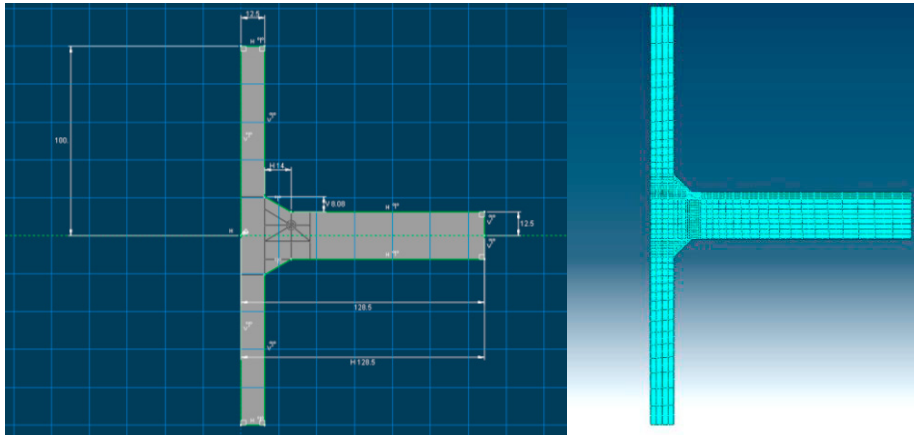


Figure 13– Model used in the simulation: dimension in mm.

In order to determine the SIFR for other values of plate thickness or variation of applied stress, it's easy to re-determine $\Delta\sigma$ and to multiply the ratio $\Delta\sigma / 150$ MPa by the table's values. In **Figure 14** it is shown how the SIFR as a function of crack depth is varying for various opening angles 2β .

Table 3- Value of K in function of crack depth from Matlab Code (tensile load case with $\Delta\sigma=150$ MPa and angle $2\beta=135$ degrees)

Crack depth [mm]	K [MPa \sqrt{m}]
0.1	8.053 (equivalent K , by BIE analysis)
0.2	8.910 (equivalent K , by BIE analysis)
0.5	10.451 (equivalent K , by BIE analysis)
1	12.00 (equivalent K , by BIE analysis)
2	14.22 (equivalent K , by BIE analysis)
3	19.57
5	28.77
7	40.05
10	66.28
12	80.98
15	130.44

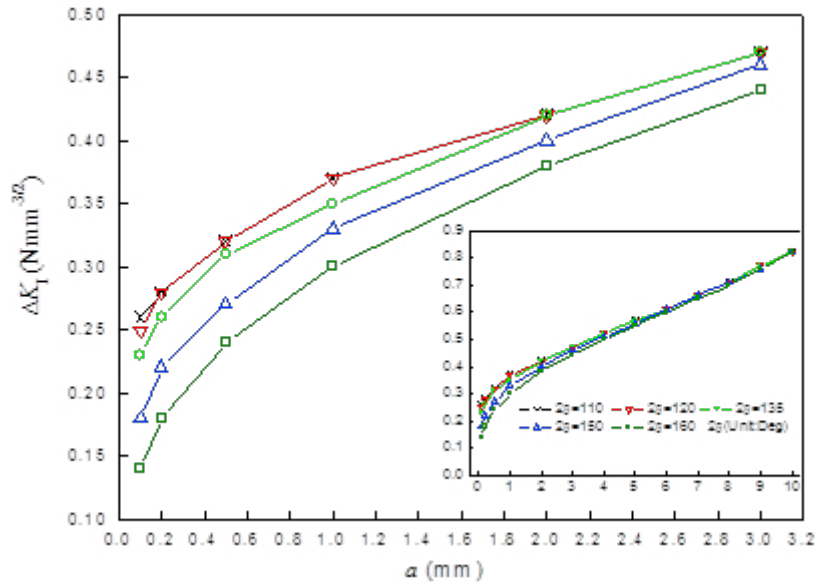


Figure 14- SIFR for the fillet weld as a function of crack depth for various values of the angle 2β

Determining the material parameters m and C in the Paris law

The measured crack growth rate in Figure 11 was analyzed as a function of the SIFR obtained by the V-notch model in Table 3. A fit based on two line segments was chosen as this gave a much closer fit to the experimental facts. The results are shown in Figure 15 for very short crack depths (from $a=0.05$ to 0.5 mm) and in Figure 16 for larger crack depths (from $a=0.5$ to 2 mm). The obtained parameters for the two cases are (median values):

Slope $m = 4.74$ and an intercept C of $771 \cdot 10^{-12}$

Slope $m=3.06$ and an intercept C of $1.065 \cdot 10^{-12}$

It is interesting to note that for small crack growth in Figure 15 no crack retardation is observed for small values of SIFR. The values in Figure 16 are quite close to what is found in the literature; however the C values are somewhat lower. This is due to the fact that the early crack growth is related to crack propagation of semi-elliptical shaped cracks that have a somewhat lower SIFR than the edge-crack in the present V-notch model. This can easily be taken into account by adding the Newman Raju multiplication factor to the present SIFR. As can be seen the correlation factor is found between 0.7 and 0.75. It should be noted that the scatter observed in Figure 16 is typical inter-specimen variation caused by different weld toe angle from specimen to specimen. As can be seen the data points are surprisingly close to a straight line for one single specimen. If for example the lower curve in figure 16 had been plotted with a more correct increased angle 2β (less steep toe angle) the curve would have been pushed upwards towards the sample mean. Hence, the large scatter in figure 16 does not reflect the scatter in the parameter C alone but also toe angle changes from specimen to specimen. All these aspects will be envisaged in future work.

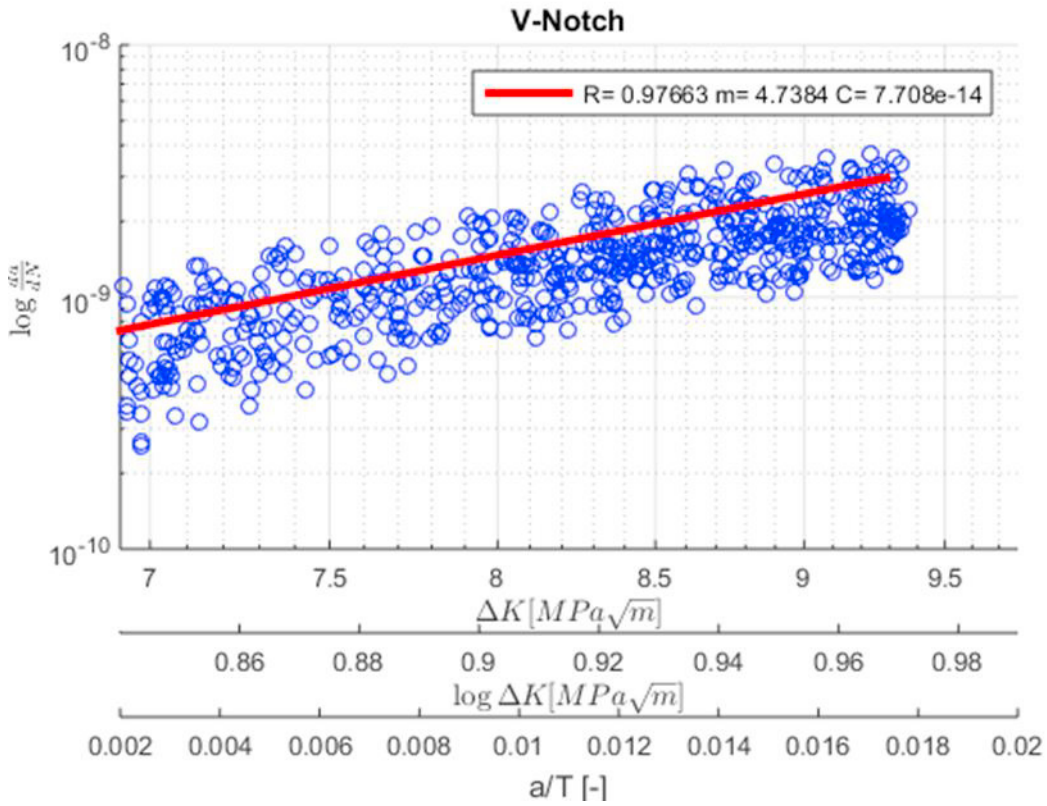


Figure 15 Crack growth in first stage from 0.05 mm to 0.5 mm.

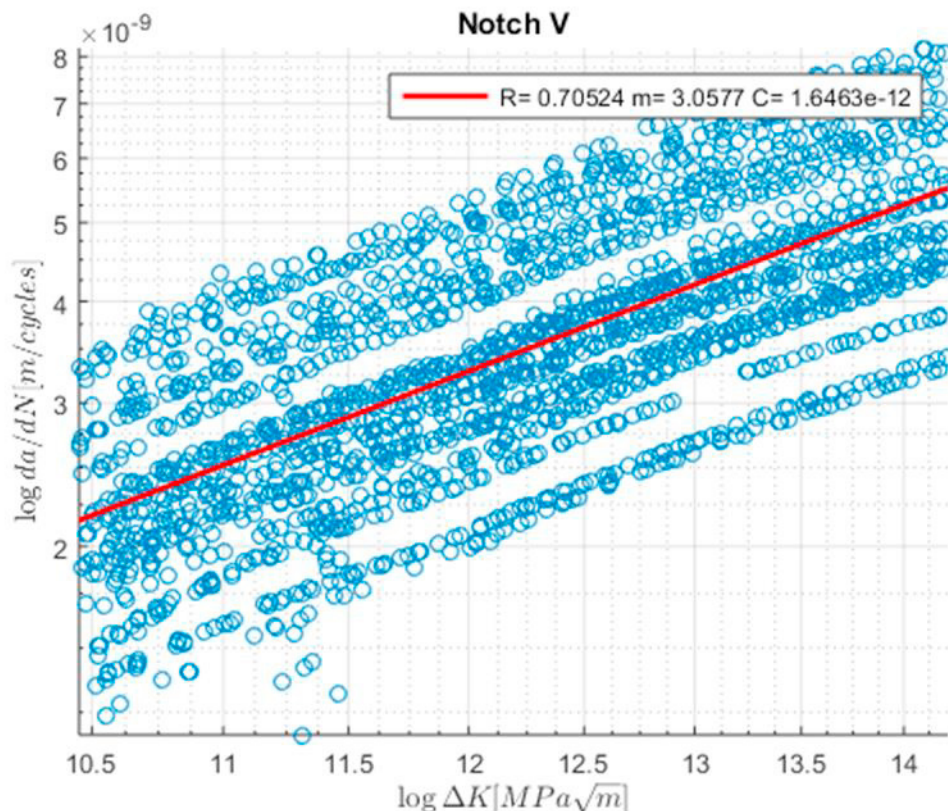


Figure 16 Crack growth from 0.5 mm to 2 mm

IV Conclusions

A V-notch approach for determining the SIFR for small crack at the weld toe has been presented. The model has been fitted the crack growth experimental data from full scale fillet welded joints where measurements of the very early growth of small cracks are available (see figure 12). It is in particular this crack regime with crack depths between 0.05 mm and 0.5 mm that the present V notch approach can determine the SIFR more correctly and with higher accuracy than the classical approaches. The SIFR associated to these small crack depths are outside the validity range for classical approaches. Furthermore, this important small crack growth regime constitutes an important part of the fatigue life of a high quality welded joint. It is also an important model for explaining the very long lives observed for welded joints near the fatigue so called fatigue limit. And it is probably the most important crack depth regime for in-service stress spectra.

References

- Atzori, B., P. Lazzarin, G. Meneghetti and M. Ricotta (2009). "Fatigue design of complex welded structures." *International Journal of Fatigue* **31**(1): 59-69.
- Bowness, D. and M. M. K. Lee (2000). "Prediction of weld toe magnification factors for semi-elliptical cracks in T-butt joints." *International Journal of Fatigue* **22**(5): 369-387.

- Carpinteri, A. and M. Paggi (2014). "The effect of crack size and specimen size on the relation between the Paris and Wöhler curves." *Meccanica* **49**(4): 765-773.
- Cheng, C., Z. Niu and N. Recho (2013). "Analysis of the stress singularity for a bi-material V-notch by the boundary element method." *Applied Mathematical Modelling* **37**(22): 9398-9408.
- Cheng, C., N. Recho, Z. Niu and H. Zhou (2011). "Effect of notch dimension on the fatigue life of V-notched structure." *Nuclear Engineering and Design* **241**(9): 3573-3579.
- Goyal, R. and G. Glinka (2013). "Fracture mechanics-based estimation of fatigue lives of welded joints." *Welding in the World* **57**(5): 625-634.
- Griffith, A. A. (1921). "The Phenomena of Rupture and Flow in Solids." *Philosophical Transactions of the Royal Society of London. Series A, Containing Papers of a Mathematical or Physical Character* **221**: 163-198.
- Gurney, T. R. and S. J. Maddox (1973). Proposed Fatigue Design Stresses for Weld Metal. R. R/RB/E56/73, Welding Institute.
- Hobbacher, A.(1993)."Stress intensity factors of welded joints." *Engineering Fracture Mechanics* **46**(2): 73-182.
- Kainuma, S. and T. Mori (2006). "A fatigue strength evaluation method for load-carrying fillet welded cruciform joints." *International Journal of Fatigue* **28**(8): 864-872.
- Labesse, F. and N. Recho (1998). "Local - Global Stress analysis of fillet welded joints." *International Institute of Welding Document IIW Doc XIII* 1737 - 1758.
- Lahti, K. E., H. Hanninen and E. Niemi (2000). "Nominal stress range fatigue of stainless steel fillet welds — the effect of weld size." *Journal of Constructional Steel Research* **54**: 161–172.
- Lassen, T. (1990). "The Effect of the Welding Process on the Fatigue Crack Growth." *WELDING RESEARCH SUPPLEMENT*: 75-82.
- Lassen, T. and N. Recho (2009). "Proposal for a more accurate physically based S–N curve for welded steel joints." *International Journal of Fatigue* **31**(1): 70-78.
- Lazzarin, P., Lassen, T. and Livieri, P. (2003). "A notch stress intensity approach applied to fatigue life predictions of welded joints with different local toe geometry." *Fatigue & Fracture of Engineering Materials & Structures* **26**(1): 49-58.
- Lazzarin, P. and P. Livieri (2001). "Notch stress intensity factors and fatigue strength of aluminium and steel welded joints." *International Journal of Fatigue* **23**(3): 225-232.
- Lazzarin, P. and R. Tovo (1998). "A notch intensity factor approach to the stress analysis of welds." *Fatigue & Fracture of Engineering Materials & Structures* **21**(9): 1089-1103.
- Lebaillif, D. (2006). *Fissuration en fatigue des structures mécano-soudées soumises à un environnement mécanique complexe*. Ph. D. Blaise Pascal University Clermont II, France (In French)

Lindroth, P., G. Marquis and G. Glinka (2013). "Fatigue crack growth of arbitrary planar cracks in welded components." Welding in the World **57**(3): 425-435.

Nykänen, T., G. Marquis and T. Björk (2007). "Fatigue analysis of non-load-carrying fillet welded cruciform joints." Engineering Fracture Mechanics **74**(3): 399-415.

Pang, H. L. J. (1991). A literature review of stress intensity factor solutions for a weld toe crack in a fillet welded joint. National Engineering Laboratory. Glaskow. **Report N°721**.

Paris, P. and F. Erdogan (1963). "A Critical Analysis of Crack Propagation Laws." Journal of Basic Engineering **85**(4): 528-533.

Recho, N. (2010). "Étude du comportement à la fatigue des assemblages soudés en fonction des effets d'entailles." Matériaux & Techniques **98**(4): 269-277.(In French)

Recho, N. (2012). Fracture Mechanics and Crack Growth, John Wiley & Sons, Inc.: 87-186.

Recho, N., L. Chin Foo, M. Faraldi and T. Lassen (2014). "Fatigue Design of Cruciform Joints including V-notch Effect at the Weld Toe." Procedia Materials Science **3**(0): 97-103.

Rice, J. R. (1968). "A Path Independent Integral and the Approximate Analysis of Strain Concentration by Notches and Cracks." Journal of Applied Mechanics **35**(2): 379-386.

Seweryn, A. (1998) A non-local stress and strain energy release rate mixed mode fracture initiation and propagation criteria. *Engng. Fract. Mech.* **59**, 737–760.

Tovo, R. and P. Lazzarin (1999). "Relationships between local and structural stress in the evaluation of the weld toe stress distribution." International Journal of Fatigue **21**(10): 1063-1078.

Williams, M. L. (1952). "Stress singularities resulting from various boundary conditions in angular corners of plates in extension." Journal of Applied Mechanics **19**: 526-528.

Yamamoto, N., M. Mouri, T. Okada and T. Mori (2012). "An analytical and experimental study on the thickness effect of fatigue strength." International Institute of Welding Document XIII(2434).